Soft Matter

Bioengineering Tunable Porosity in Bacterial Nanocellulose Matrices

Journal:	*Soft Matter*
Manuscript ID	SM-ART-09-2019-001895.R1
Article Type:	Paper
Date Submitted by the Author:	25-Oct-2019
Complete List of Authors:	Ashrafi, Zahra; North Carolina State University, Fiber & Polymer Science Krause, Wendy; NC State University, College of Textiles Lucia, Lucian; North Carolina State University, Department of Forest Biomaterials; Qilu University of Technology,

Bioengineering Tunable Porosity in Bacterial Nanocellulose Matrices

Zahra Ashrafi†, Lucian Lucia‡†§*, Wendy Krause†

†Fiber and Polymer Science, NC State University, Campus Box 7616, Raleigh, North Carolina 27695, United States

‡Department of Forest Biomaterial, NC State University, Campus Box 8005, Raleigh, North Carolina 27695, United States; Department of Chemistry, NC State University, Campus Box 8204, Raleigh, North Carolina 27695, United States

§State Key Laboratory of Bio-based Materials & Green Papermaking, Qilu University of Technology / Shandong Academy of Sciences, Jinan, PR China 250353

*lalucia@ncsu.edu

Abstract

A facile and effective method is described to engineer original bacterial cellulose fibrous networks with tunable porosity. We showed that the pore shape, volume, and size distribution of bacterial nanocellulose membranes can be tailored with appropriate culture conditions specifically carbon sources. Pore characterization techniques such as capillary flow porometry, bubble point method, gas adsorption-desorption technique as well as visualization techniques such as scanning electron and atomic force microscopy were utilized to investigate the morphology and shapes of the pores within the membranes. Engineering the various shape, size and volume characteristics of the pores available in pristine bacterial nanocellulose membranes lead to fabrication and development of eco-friendly materials with required characteristics for a broad range of applications.

1. Introduction

Several species of microbes, most noteworthy among them is *Gluconacetobacter*, have an ability to extracellularly grow a nanoscale cellulosic matrix on the interface of air-liquid medium in stationary cultures. The grown three-dimensional (3D) nanostructured matrices are a pure biopolymer composed of very fine, 40−60 nm diameter, ribbon-shaped cellulose nanofibers which are about 200 times finer than cotton fibers and exhibit a remarkable high surface area.[1,2,3,4,5] Moreover, Bacterial cellulose (BC) membrane has exceptional flexibility; meanwhile, shows high tensile strength (200−300 MPa), higher degrees of polymerization and crystallinity than plant cellulose, high thermal and chemical stability, and high absorption capacities.[3,6,7] These properties make bacterial nanocellulose superior for a variety of applications including textiles, food products, flexible electronics and optics, supercapacitors, diagnostic sensors, and cosmetics.[8,9,10,11,12,13]

More importantly, the microstructure of bacterial cellulose mimics the extracellular matrix of human skin; thus, they are promising candidates for medical applications such as wound dressings and soft tissue engineering.[14,15,16] However, the tight network of cellulose nanofibrils can hinder their performance and limit cell infiltration.[17,18] Improving the porosity of the native BC membrane is critical not only for developing novel functional biomaterials that can give rise to artificial organs and tissue scaffolds designs, but also for immobilizing and the storage of various compounds such as enzymes, drugs, etc., and also for separations, sorption, and catalytic purposes.[19,20,21,22,23,24]

In this regard, past work has tried to alter the porosity of BC networks by employing particle-leaching technique.[25] The technique consists of introducing foreign substrates such as solid particles of paraffin and potato starch into the structure of the BC matrices during cultivation, followed by leaching to extract the solid particles residue from the materials.

Still the particle-leaching techniques face serious issues; first, removing the residue of solid particles trapped into the bulk structure of the BC membrane is challenging and tedious and, in some cases, results in fractured pore structures. Second, it does not maintain the intrinsic microporous structure of the native BC membrane which show similarities to the extracellular matrix (ECM) components of the human body and thus, it is critical that it remain unchanged for medical applications.[26] Third, it causes negative effects on the strength of the membrane by destroying the BC fibrous structure. In this respect, finding a way to enhance the pore volume in the native bacterial nanocellulose matrices, which provides the dominant contribution to improve surface area and control the migration and transportation of cells, solid particles, fluids, and so forth, is of great importance.

Herein, the current work showed that culture conditions, specifically applying different types of carbon sources can be employed to tune overall porosity and morphology of bacterial nanocellulose matrices including pore shapes, size, volume distributions and fluid permeability behavior without sacrificing the inherent bio-architecture. Moreover, it has been found that the transparency of the BC pellicles can be altered significantly by growth media carbon components. Capillary flow porometry, bubble point method, gas adsorption-desorption techniques, as well as visualization techniques such as Field Emission Scanning Electron

Microscope (FESEM) and Atomic Force Microscopy (AFM) were utilized to characterize the pores as well as air and fluid permeability properties of each membrane.

2. Experimental

2.1 Materials

Gluconacetobacter hansenii was purchased from American Type Culture Collection ATCC® 23769™. Mannitol, yeast extract, bacto-peptone (becton, Dickinson and Company), di-sodium phosphate, and citric acid were used for preparing the appropriate culture media. Hydrogen chloride and potassium hydroxide solution 1N (N/10), were used to purify membranes. All the reagents were purchased from Sigma-Aldrich and used as received unless otherwise stated.

2.2 Preparation of Bacterial Cellulose Membranes

The medium for inoculation preparation and membrane formation consists of the following (v/v): carbon source (glucose, mannitol, fructose, sucrose, or glycerol) 2%, peptone 0.3%, yeast extract 0.5%, dibasic sodium phosphate 0.27%, citric acid 0.114%. The cultivation medias were autoclaved at 121℃ for at least 15 minutes before proceeding.

Fermentation cultures for each carbon sources performed in 6-well plates containing 10 ml of fresh above medium with 5% (v/v) cell suspension media. All five 6-well plates were incubated statically under atmospheric conditions at 30℃ for 10 days to BC membranes form. To remove

non-cellulose materials, the samples were immersed in 1M KOH solution at room temperature for 48 hours. After this time, BC membranes were transferred to HCl 0.5M bath to neutralize the base. After an hour of neutralization, the cellulose was rinsed repeatedly in DI water until shows neutral pH. Finally, the membrane was stored in fresh DI water at 4℃ for further experiments.

2.3 Morphology Characterization

Surface and bulk morphology of freeze-dried BC membranes were observed by Field Emission Scanning Electron Microscopy (FEI Verios 460L, FESEM). Samples were gold-palladium (50:50) coated (~15 nm thickness) with Technics Hummer V Sputter Coater to reduce charge interruptions before taking FESEM images.

The density (g/cm^3) of dry samples was measured by measuring the mass and volume of freeze-dried samples using below equation:

$$Density = {}^{M}/_{V}$$

where M is the sample weight (g) and V is the sample volume (cm^3).

2.4 Pore Size Characterization

Capillary Flow Porometry and Bubble Point test (Porous Materials Inc, CFP-1100_AEL) were used to measure the flow pore diameter distribution along with the bubble point within the

obtained membranes. The samples were dried in a freeze-dryer at < 50 Pa and -50°C for at least 48 h without any pre-freezing to maintain pore structures. Subsequently, a fully wetted sample in Galwick solution with known surface tension of 15.9 Dynes/cm, was placed in the sample chamber and the chamber was sealed. Nitrogen gas was then allowed to flow into the chamber behind the sample.

The bubble point has been found when the pressure reaches a point that can overcome the capillary action of the fluid within the largest pore. The bubble point is defined by the ASTM F-316-03 standard as the pressure at which the first continuous gas bubbles is detected. After determination of the bubble point, the pressure was continuously increased, and flow was measured until all pores were empty from Gatwick solution. At that point, the sample was considered dry by the instrument and the air flow though the sample was recorded.

To further investigate the through pores within the membrane, 200 ml of deionized water was passed across the membrane under gravity. The pure water flux (J, $L.m^{-2}.h^{-1}$) was calculated as follows:

$$J = {}^{V}/_{(A \times t)}$$

where V is the volume of the water filtered (L), A is the effective filtration membrane area (m^2), and t is the filtration time (h).

Moreover, porosity and surface area of the membranes were determined by the analysis of nitrogen adsorption-desorption analysis (Micrometrics 3FLEX Surface Characterization, Version 4.04).

2.5 Surface Roughness

Atomic force microscopy (AFM), with a very-high-resolution in a non-contact mode was used to scan freeze-dried samples area to accurately characterize and visualize the variation of surface microstructures.

3. Results & Discussions

3.1 Morphology Characterization

By playing with culture conditions, altering cellulose pellicle (mat) properties is possible.[1,27,28,29] The main nutrient for the bacteria is sugar. A single bacteria cell can polymerize 100 glucose molecules into cellulose within an hour. Because the *Gluconacetobacter* bacteria are obligate aerobes, many synthesized fibrils, suspended in the inoculation medium, gradually form a randomly-assembled fibrous metrics that floats at the air/liquid interface.[30,31] Five different types of carbon sources were applied in growth culture with all other conditions constant. Results showed all carbon sources supported growth of the bacteria strain (Figure 1 A). While under the same cultivation circumstances, each carbon source results in a membrane with different

thickness and density; moreover, glycerol and fructose gave the highest cellulose yields of 2.05 and 1.82 $g.L^{-1}$, respectively.

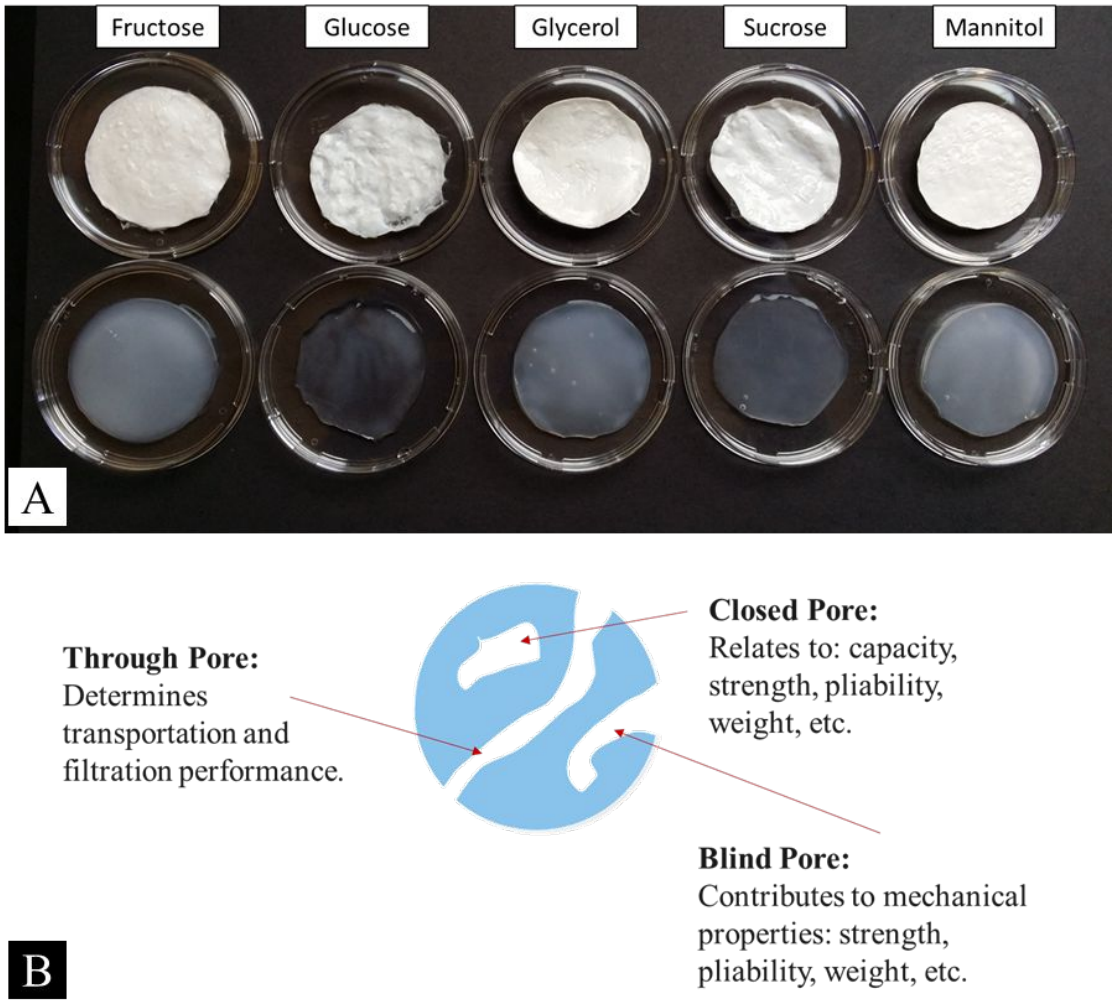

Figure 1. (A) Bacterial cellulose membranes by applying different types of carbon sources in growth culture with all other conditions constant. Top row; freeze dried samples without pre-freezing which locks the porous structure in place. Bottom row; samples in water infused state. (B) Schematic of pores classification according to their availability to surroundings.

In general, there are different types of pores in fibrous membranes as shown Figure 1 B: one which is known as through-pores is accessible at two external surfaces of the membrane and travel all the way through the membrane, commonly evaluated for pore size measurements. There are also blind or dead-end pores which are open at one end, but do not participate in the permeability of the membrane and are subject to adsorption and desorption of particles and living cells. Closed pores are types of the pores that are trapped and encapsulated inside the materials and have no access to external surfaces; thus, they are not associated with any absorption or transportation, but still important in terms of mechanical properties such as strength, pliability, and weight.[32,33]

Fluid permeation behavior can be attributed to through pores which are the only form of pores that participate in the transportation of matter. Higher fluid movement through the samples clearly point out either more or larger size distribution transportation pores. Therefore, the gravity-driven water flux through each sample was carried out with a dead-end filtration assembly as a tool to further study the permeation behavior and membrane morphology.

Results are shown in Figure 2 and Table S1. Glycerol shows the highest water flux with a significant difference compare to other carbon sources followed by fructose, sucrose, mannitol, and glucose. Gravity-driven water flux assessments showed that glycerol improves fluid flux by 32% relative to fructose, which was the next best flux system, thus offering the most energy-efficient membrane for permeability and separation applications.

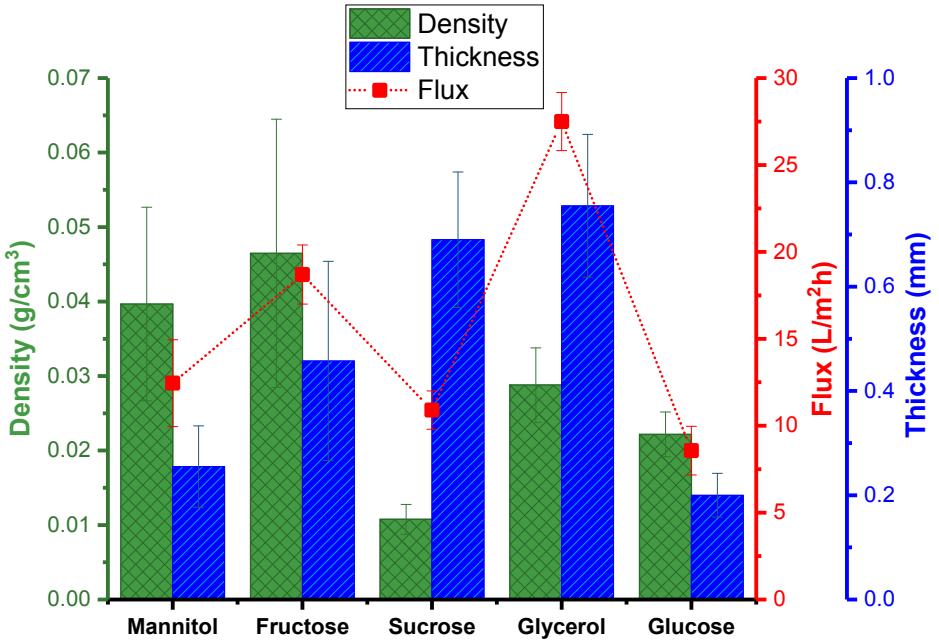

Figure 2. Effect of different types of carbon sources on thickness, water flux and density of BC membranes.

FESEM inspection revealed the microstructure of the bacterial membranes (Figure 3). The obvious differences between the fibrous network of the membranes confirm that the application of different types of carbon sources is an important parameter for optimizing pore volume and morphology of the BC pellicles.

As it is apparent from the images, with this bacteria strain, cylindrical pores and micro-channels of varying sizes are present in the structure of the all membranes. The size of cylindrical pores is < 1 micron. SEM images verified that among five different types of carbon sources utilized in inoculation medium, glycerol, and fructose-fed samples provide the most open structures with bigger pore size distribution.

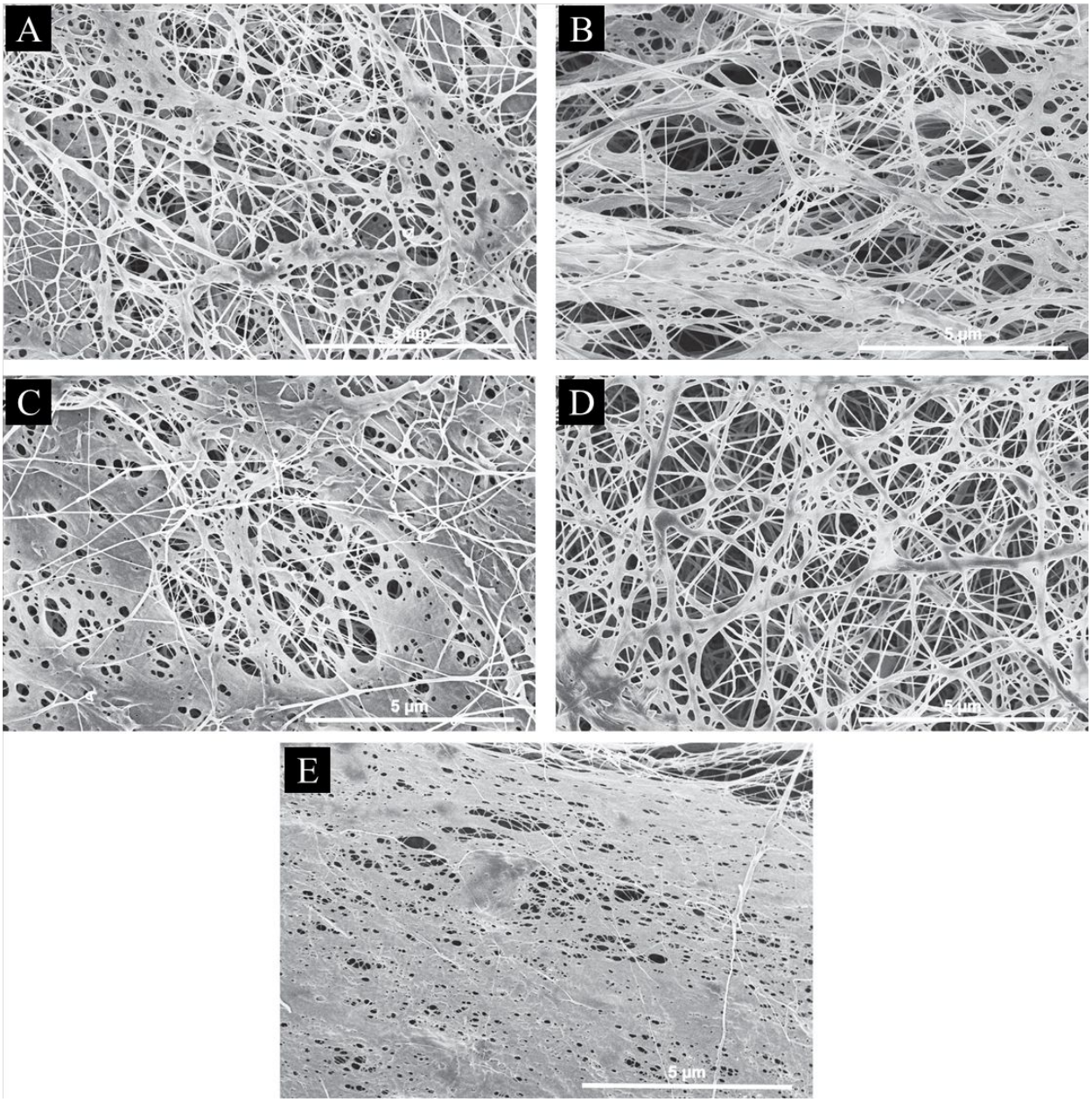

Figure 3. SEM images of BC membranes obtained by applying different types of carbon sources in growth culture with all other conditions constant: A) Mannitol. B) Fructose. C) Sucrose. D) Glycerol. E) Glucose.

3.2 Pore Size Characterization

Although SEM is a great direct assessment technique to characterize pore structures which exist in a sample, it is too much of a localized approach and thus, applying a reliable representative assessment of the whole material can be quite challenging especially for BC membranes which are natural products and tend to show significant variations in morphology. Therefore, to validate and quantify our findings on the through-pores present in the BC membranes, both Bubble Point Test and Capillary Flow Porometry techniques were used. Both of these techniques are based on the fact that there is an inverse proportion between a size of a pore wetted with a fluid with known surface tension and the required pressure to force the wetted fluid to expel from that pore.[34,35]

The Washburn Equation (based on the Young-Laplace Equation) defines the correlation between this pressure drop and the size of the capillary, or through-pore, as follows:

$$D = K\frac{4\gamma cos\theta}{P} \quad (1)$$

where D is diameter of the pore, K is a shape correction factor since in a practical membrane element are likely to be shaped like capillary tubes, γ is surface tension of the liquid, θ is liquid-solid contact angle, and P is pressure.

While the Bubble Point tests helped us to determine size of the largest through pore within the membranes, in order to understand how many through pores of different sizes are present in the

medium, an assessment of the pore size distribution was provided by Capillary Flow Porometry technique.

The results of Bubble Point tests, Figure 4, showed that among carbon sources that were fed to the bacteria, sucrose causes formation of the biggest through pore size that are significantly different to other carbon sources, followed by fructose, mannitol, glycerol, and glucose. However, as mentioned earlier, this measurement corresponds to the largest or maximum pore size available in the membranes, yet other through pore characteristics, such as size distribution, shape and tortuous nature determine the overall permeability and release profile associated with the membranes. The results of Capillary Flow Porometry test, Figure 4 and Table S2, illustrate that the presence of glycerol and fructose in growth culture resulted in membranes with higher mean through pore size along with lower mean flow pore pressure. The Capillary Flow Porometry test results show broad standard deviation values which feature the significant variation that natural products inherently exhibit. The remarkable distinction of inner microstructure of these naturally occurring samples require employing different techniques to assess porosity specifically vertical pore size and permeability properties of these samples.

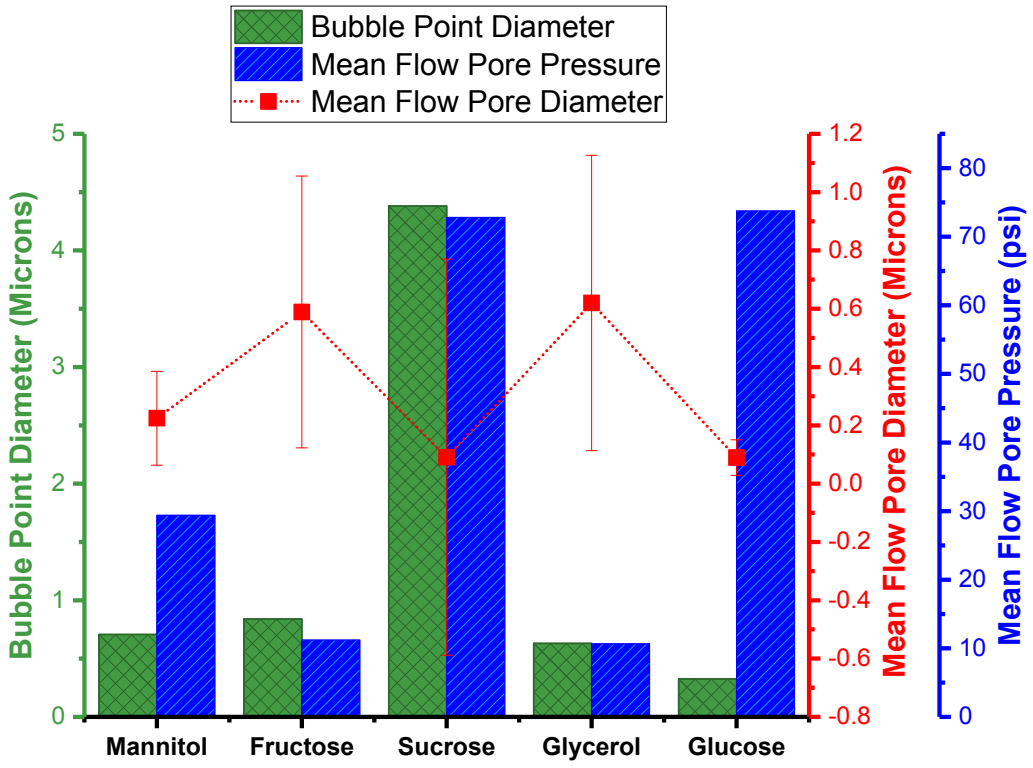

Figure 4. Results of Bubble Point and Capillary Flow Porometry tests on BC membranes obtained from different carbon sources.

Although both glycerol and fructose-fed samples show around the same mean diameter for flow pores, but glycerol-fed samples showed around 32% greater water flux over fructose-fed samples (Figure 6). To better understand the underlying reasons behind this, we need to consider pore size distribution for each sample which provides a quantitative description of the range of pore sizes present in a given membrane and is obtainable from Capillary Flow Porometry based on the following equation:

$$f = -d[(\frac{fw}{fd}) \times 100]/dD \quad (2)$$

where f is pore distribution, f_w is flow rate through wet sample, f_d is flow rate through dry sample, and D is pore diameter.

The data obtained from Capillary Flow Porometry experiments clearly indicate that the glycerol-fed sample has larger pore sizes compare to the fructose-fed sample while the mean pore size for both is around the same. There is a wider range of pore sizes in the fructose-fed sample. In fact, a lot of pores in this samples fall within the range of 0.2-0.22 microns (Figure 5A). Moreover, if we study the flow rate behavior of each sample under pressure, before 50 psi both samples approximately show the same behavior however, the flow rate of air/liquid through glycerol-fed samples soar up after that pressure (Figure 5B). One possible explanation might lie in the tortuosity structure of inner pores. The small inner pores might be connected to each other through micro-sized channels which are generally very hard to determine with common techniques. Under high pressure these micro channels might explode and result in an exponential increase in the flux of glycerol-based membranes.

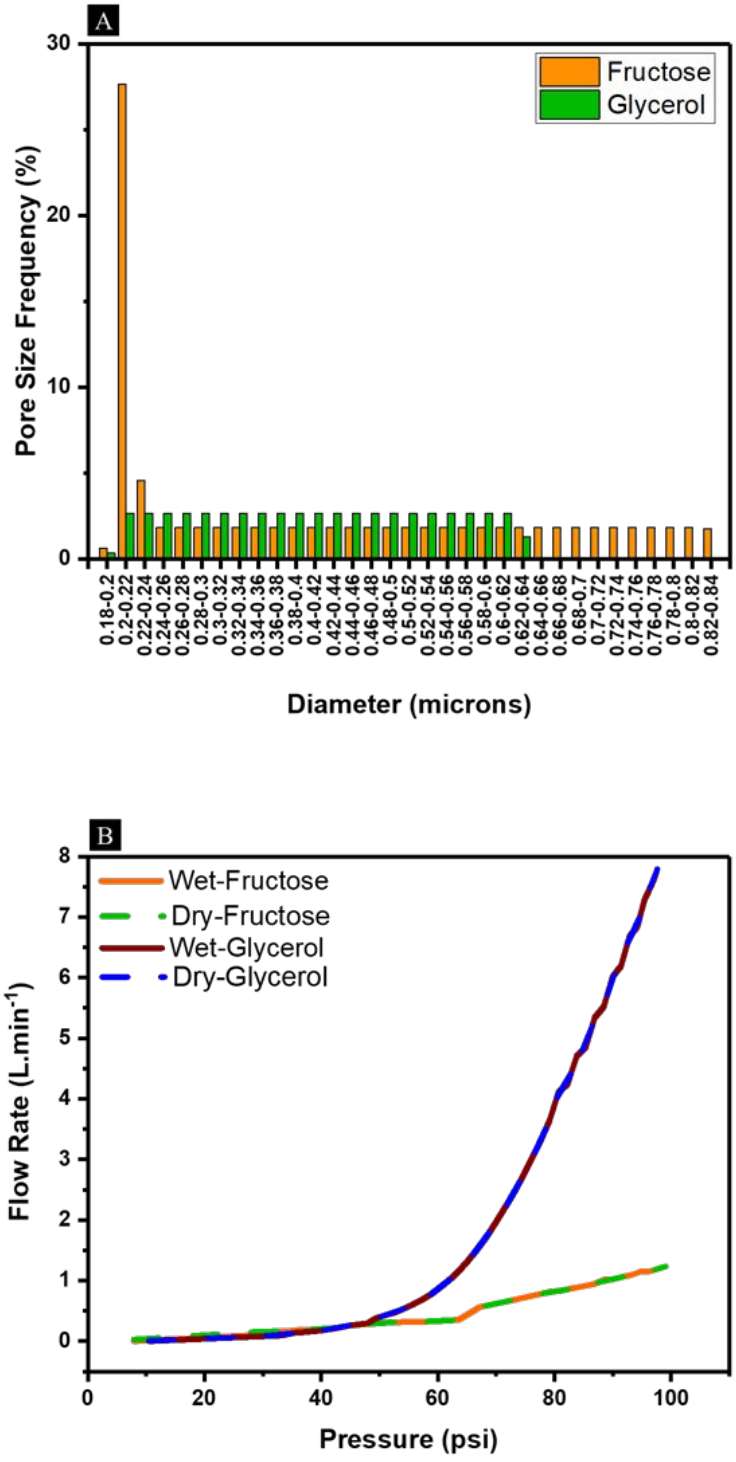

Figure 5. A) Pore size distribution for glycerol and fructose fed BC membranes obtained from Capillary Flow Porometry test. B) Wet/dry flow rate behavior of glycerol and fructose fed BC membranes under pressure.

We also measured the density of glycerol and fructose-fed samples and realized that fructose-fed samples are denser than glycerol-fed samples; thus, by deduction, because both samples have about the same average size of through pores, the overall pore volume must be higher in glycerol-fed sample (Figure 7). It is worth noting, while the pore dimeter varies along a single pore, Capillary Flow Porometry measures the most restricted pore diameter along a pore path, therefore, it is incapable of assessing pore volume data accurately.

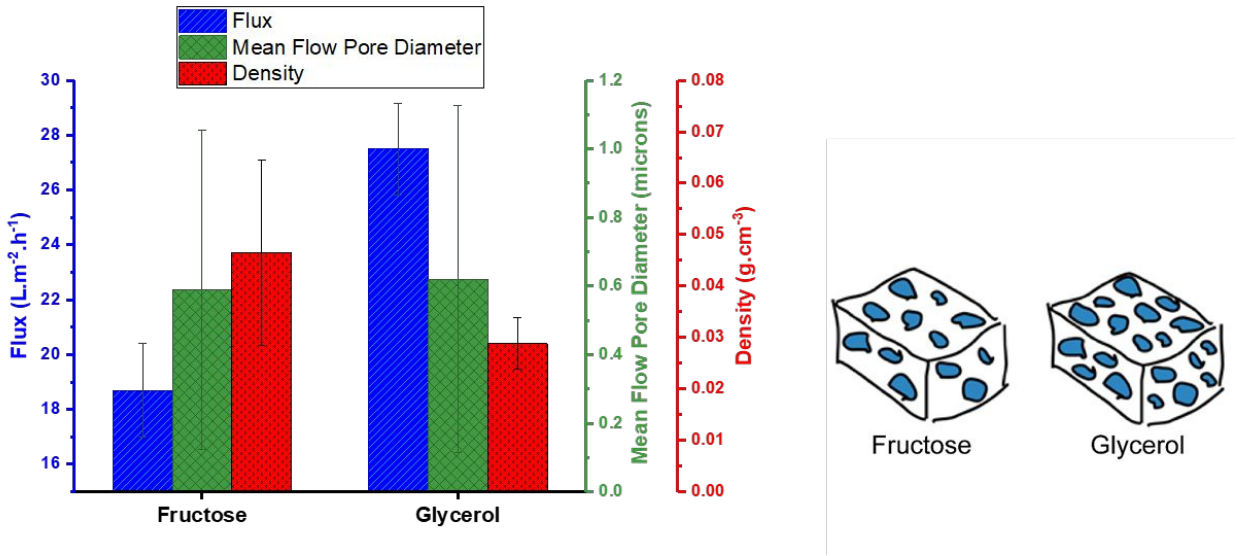

Figure 6. Results of water flux, mean flow pore diameter, and density for glycerol and fructose-fed BC membranes and schematic illustration of BC membrane structure cultivated with two carbon sources glycerol (right) and fructose (left).

While it is out of the scope of the current work, to answer why modulating a carbon component of bacteria growth medium can lead to variability in cellulose production behavior of bacteria which subsequently affects the nanocellulose membrane inner structure, it should be pointed out that the starting pH value of all inoculation medias were adjusted the same (4.5). However,

recorded pH, after 7 days of inoculation were quite different as presented in Table 1 depending on which carbon source is used. It has been shown that the pH outside the bacteria affects the overall structure and permeability of the bacteria cell membrane, which can influence cellulosic network formation. There might be no gluconic acid production during glycerol metabolism, thus pH remains stable which provided a favorable breeding ground for bacterial growth. Whether this is the principal reason for the great difference in nanocellulose network morphology remains unclear. Moreover, a cultivation pH below 3 results in no production of cellulose and the proliferation of the bacteria are negatively affected; therefore, glucose is the least desirable among the options in this regard.[31]

Another aspect of this is bacteria consume carbon sources to obtain energy. Rapidly utilized energy sources can lead to changes on the enzymatic pathway to cellulose production and network formation. Thus, studying the by-products produced by consuming various energy sources during BC production can be very helpful in this regard. Several attempts to improve BC production by maintaining optimal pH have been reported.[36,37,38]

Table 1. pH of bacterial nanocellulose growth medias with different carbon substrates after 7 days of inoculation

	Mannitol	**Fructose**	**Sucrose**	**Glycerol**	**Glucose**
pH	6.1±0.3	5.8±0.4	6.0±0.2	6.2±0.3	4.2±0.3

3.3 Pore Volume Characterization

Although Capillary Flow Porometry and Bubble Point techniques are quick and convenient, they are not proficient in terms of providing direct data regarding the pores volume in solid materials. In fact, both of these methods can describe the most constricted pore size of a through pore while the pore shapes are irregular in most cases. Other techniques, such as, gas adsorption/desorption, are capable to determine pore volume data from the adsorption and desorption isotherms of a gas subjected to condensation in the pores. However, it is important to remember that gas adsorption/desorption techniques are incapable of discriminating between through pores and blind pores.

Figure 7 shows the nitrogen adsorption-desorption isotherms for various BC membrane samples cultivated with applying different carbon sources in the growth media. The obtained isotherms illustrate that the quantity of adsorbed nitrogen is different for each sample. The fructose and glycerol-fed samples with higher surface area found to have higher nitrogen adsorption than the other samples. It is worth noting from the isotherms that higher surface area results in higher adsorption. The nitrogen adsorption property and surface area of the samples showed a decreasing trend in the following order: fructose > glycerol > mannitol > sucrose > and glucose.

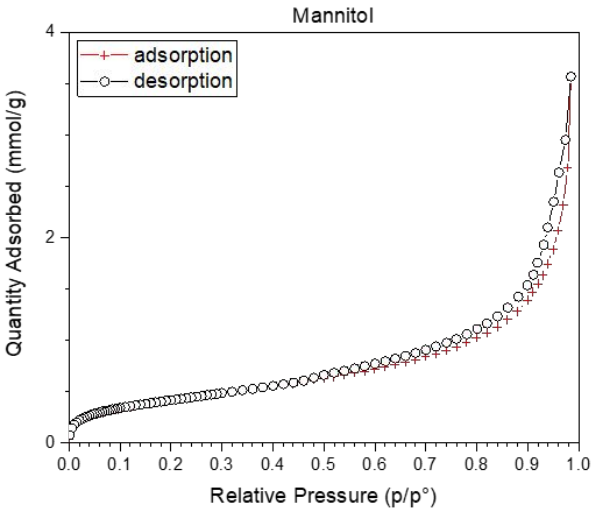
Mannitol
adsorption
desorption
Quantity Adsorbed (mmol/g)
Relative Pressure (p/p°)

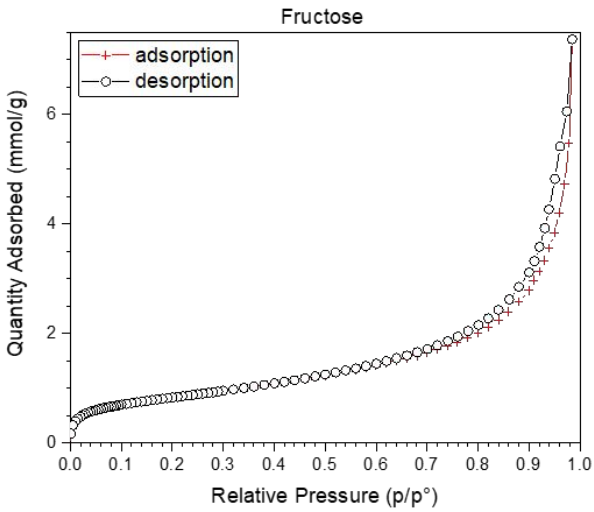
Fructose
adsorption
desorption
Quantity Adsorbed (mmol/g)
Relative Pressure (p/p°)

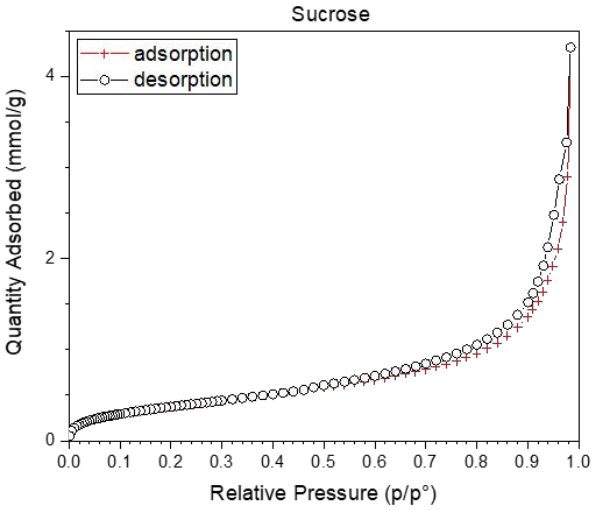
Sucrose
adsorption
desorption
Quantity Adsorbed (mmol/g)
Relative Pressure (p/p°)

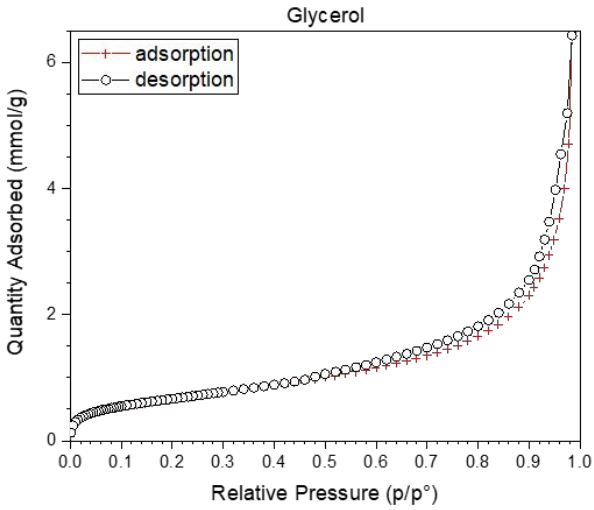
Glycerol
adsorption
desorption
Quantity Adsorbed (mmol/g)
Relative Pressure (p/p°)

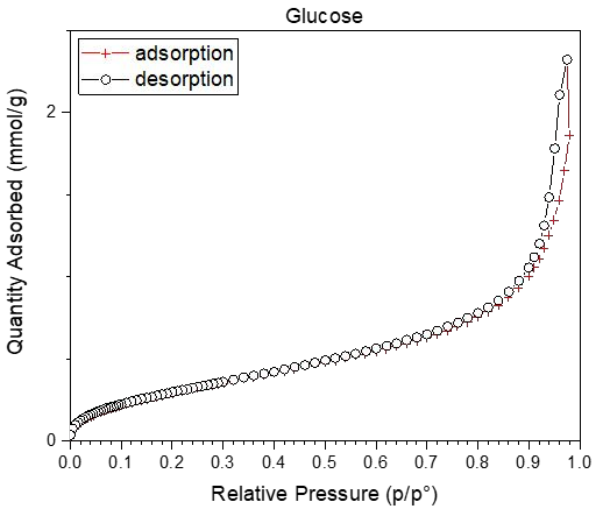
Glucose
adsorption
desorption
Quantity Adsorbed (mmol/g)
Relative Pressure (p/p°)

Figure 7. Nitrogen adsorption-desorption isotherm of BC membranes cultivated with different types of carbon sources.

The data on BET surface area, pore volume, and average pore size of the BC membranes are presented in Table 2 and Figure 8 in which the surface area and pore volume reveal the same trend. The highest surface area attributed to fructose sample with 66% higher value compared to the glucose sample with the least surface area. The pore volume results found to show a declining trend from highest, fructose, to lowest, glucose, by 56%.

Contrary to surface area and pore volume data, pore size results show an opposite trend with highest amount associated with glycerol followed by glucose and sucrose, and then mannitol and fructose samples. Considering Capillary Flow Porometry data, the glycerol sample also has the highest average through-pore size, whereas glucose and sucrose had the smallest one. However, it is important to point out that gas adsorption-desorption assess not only through-pores, but also blind pores and channels between pores which do not participate in permeability properties of BC pellicles and thus are not recognizable by flow porometry techniques.

Table 2. Brunauer, Emmett, Teller (BET) surface area, pore volume, and pore size of the BC membrane structures cultivated with five different carbon sources.

Sample	BET surface area (m^2/g)	Pore vol.[1] (cm^3/g)	Average pore diameter[2] (Å)
Mannitol	32±0.35	0.12	82
Fructose	65±0.45	0.25	82
Sucrose	31±0.16	0.15	85
Glycerol	52±0.52	0.23	88
Glucose	22±0.48	0.11	85

[1] Barrett, Joyner, Halenda (BJH) adsorption cumulative volume of pores between 17.000 Å and 3000.000 Å width
[2] Adsorption average pore width (4V/A by BET)

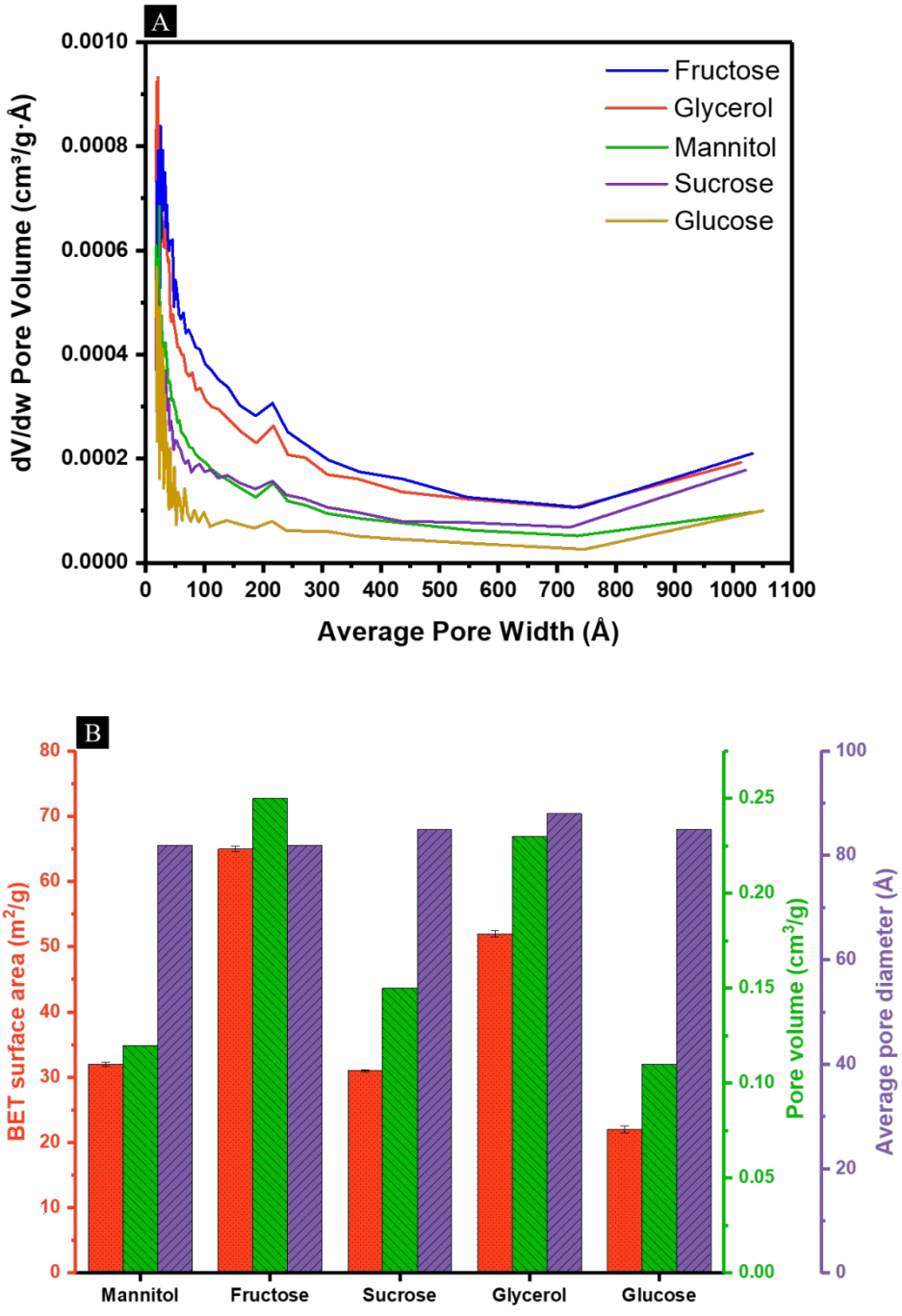

Figure 8. A) BJH pore size distribution of the BC membrane structures cultivated with five different carbon sources. B) Brunauer, Emmett, Teller (BET) surface area, pore volume, and pore size of the BC membrane structures cultivated with five different carbon sources.

3.4 Surface Roughness Characterizations

The surface of the membranes possesses a large roughness factor because of the inherent reentrant curvature of the nanofibers and microstructured pores. Atomic force microscopy (AFM) equipped with a cantilever with a nanometer-scale tip in non-contact mode was used to scan surface features and pore morphology of the samples as shown in Figure 9.

The open porous structure can clearly be seen in fructose and glycerol-fed samples, B and C, respectively. However, the porous structures gradually diminsh for the mannitol, sucrose, and glucose-fed samples. The results of root mean square (RMS) of surface roughness for all the samples at both 1- and 10-microns length scale are summarized in the table in Figure 9.

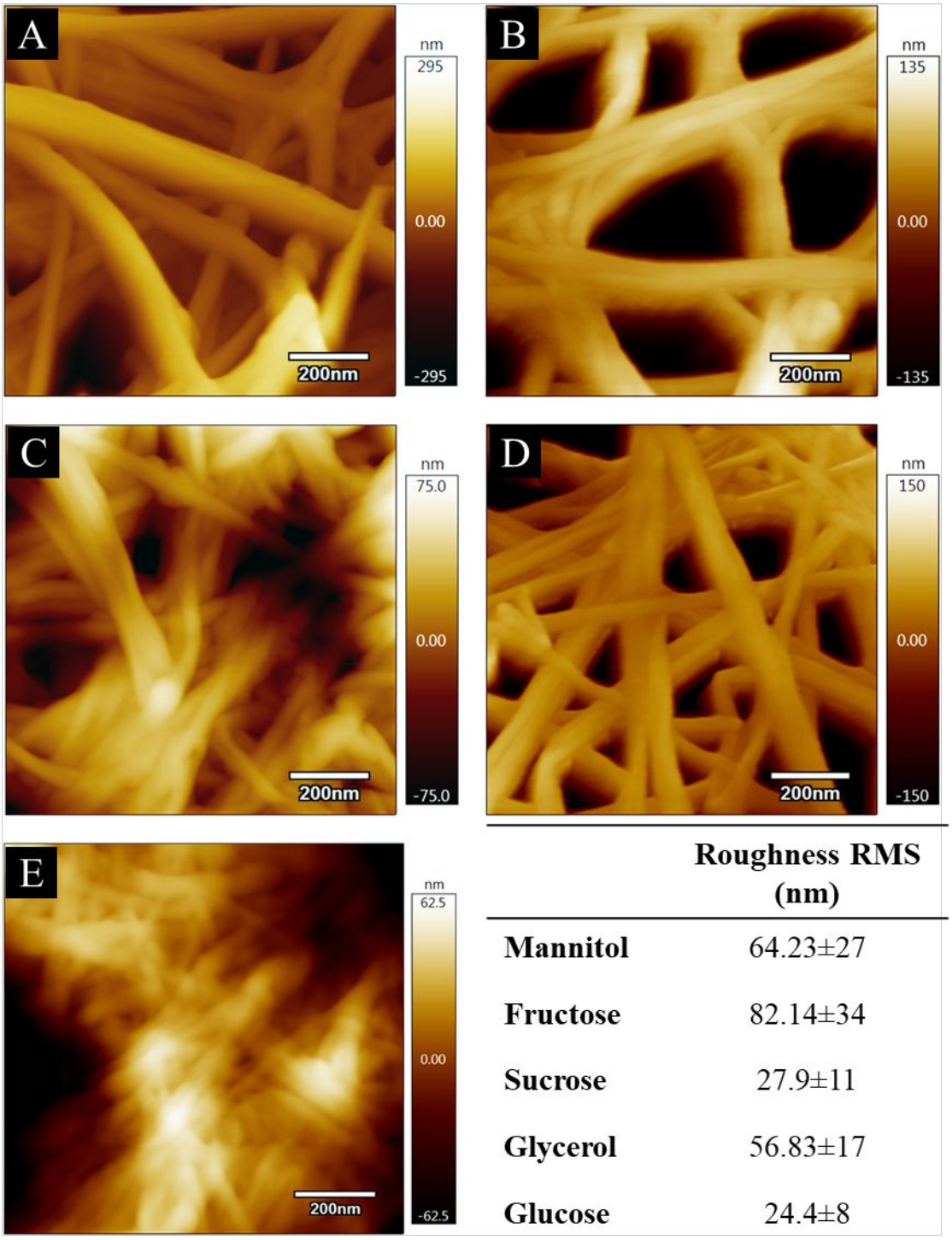

	Roughness RMS (nm)
Mannitol	64.23±27
Fructose	82.14±34
Sucrose	27.9±11
Glycerol	56.83±17
Glucose	24.4±8

Figure 9. Surface roughness of bacterial nanocellulose matrices obtained by applying different types of carbon sources in growth culture with all other conditions constant: A) Mannitol. B)

Fructose. C) Sucrose. D) Glycerol. E) Glucose. Table shows roughness root mean square (RMS) of bacterial nanocellulose matrices cultivated with five different carbon sources.

4. Conclusions

Bacterial nanocellulose membranes are promising three-dimensional nanostructured matrices and have been used for innumerable applications because of their unique green nature along with sustainable and cost-efficient production methods. However tight pore structures present in the native membrane restrict practical application. Therefore, to tailor pore size, shape and volume of original nanocellulose membranes, different types of carbon sources in growth culture were applied with all other conditions constant. Our experiments were able to demonstrate that feeding the bacteria different types of carbon sources under static culture conditions alter the morphology of the bacterial nanocellulose membrane at both the macro- and micro- scales.

Among five different types of applied carbon sources, glycerol- and fructose- fed samples result in the most porous structure with highest pore surface area. The higher inner surface area is a critical feature of the bacterial nanocellulose membranes which adjusts many fundamental properties such as mechanical and thermal stability, fluid permeability, pliability and compactability, sorption properties and even the lifecycle of materials. This work offers a simple effective method to induce porosity in native BC membrane without needing to chemically or mechanically destroying the original unique structure and crystallinity of these natural masterpieces.

Acknowledgements

We gratefully acknowledge the support of the Fiber and Polymer Science (FPS) program and the Nonwoven Institute (grant number 525667) at NC State University under whose umbrella ZA was able to pursue the work described and obtain her PhD as of this writing. We thank Dr. Manuel Kleiner and Dr. Rebecca-Ayme Hughes from the Department of Plant and Microbial Biology at North Carolina State University who provided insights and expertise that greatly assisted the execution of the research.

REFERENCES

1. Huang, Y. *et al.* Recent advances in bacterial cellulose. *Cellulose* **21**, 1–30 (2014).

2. Klemm, D., Heublein, B., Fink, H. & Bohn, A. Polymer Science Cellulose : Fascinating Biopolymer and Sustainable Raw Material. *Angew. Chemie Int. Ed.* **44**, 3358–3393 (2005).

3. Iguchi, M., Yamanaka, S. & Budhiono, a. Bacterial cellulose — a masterpiece of nature ' s arts. *J. Mater. Sci.* **35**, 261–270 (2000).

4. Lustri, W. R. *et al.* Microbial Cellulose — Biosynthesis Mechanisms and Medical Applications. in *Cellulose - Fundamental Aspects and Current Trends* 133–157 (IntechOpen, 2015). doi:10.5772/61797

5. Ashrafi, Z., Mazinani, S., Ghareaghaji, A. A. & Lucia, L. Fabrication of cross-linked starch-based nanofibrous mat with optimized diameter. *TAPPI J.* **18**, 381–389 (2019).

6. Penttilä, P. A., Sugiyama, J. & Imai, T. Effects of reaction conditions on cellulose structures synthesized in vitro by bacterial cellulose synthases. *Carbohydr. Polym.* **136**, 656–666 (2016).

7. Watanabe, K., Tabuchi, M., Morinaga, Y. & Yoshinaga, F. Structural Features and Properties of Bacterial Cellulose Produced in Agitated Culture. *Cellulose* **5**, 187–200 (1998).

8. Li, G. *et al.* An environmentally benign approach to achieving vectorial alignment and high microporosity in bacterial cellulose/chitosan scaffolds. *RSC Adv.* **7**, 13678–13688 (2017).

9. Chen, X. *et al.* Recent approaches and future prospects of bacterial cellulose-based

electroconductive materials. *J. Mater. Sci.* **51**, 5573–5588 (2016).

10. Svensson, A. *et al.* Bacterial cellulose as a potential scaffold for tissue engineering of cartilage. *Biomaterials* **26**, 419–431 (2005).

11. Dayal, M. S. & Catchmark, J. M. Mechanical and structural property analysis of bacterial cellulose composites. *Carbohydr. Polym.* **144**, 447–453 (2016).

12. Liu, F., McMaster, M., Mekala, S., Singer, K. & Gross, R. A. Grown Ultrathin Bacterial Cellulose Mats for Optical Applications. *Biomacromolecules* **19**, 4576–4584 (2018).

13. Ashrafi, Z., Lucia, L. & Krause, W. Nature-Inspired Liquid Infused Systems for Superwettable Surface Energies. *ACS Applied Materials and Interfaces* **11**, 21275–21293 (2019).

14. Wojciech K. Czaja, †, ‡, David J. Young, †, Marek Kawecki, § and & R. Malcolm Brown, J. . The Future Prospects of Microbial Cellulose in Biomedical Applications. *Biomacromolecules* **8**, 1–12 (2006).

15. Petersen, N. & Gatenholm, P. Bacterial cellulose-based materials and medical devices: Current state and perspectives. *Appl. Microbiol. Biotechnol.* **91**, 1277–1286 (2011).

16. Moniri, M. *et al.* Production and Status of Bacterial Cellulose in Biomedical Engineering. *Nanomaterials* **7**, 1–26 (2017).

17. Zaborowska, M. *et al.* Microporous bacterial cellulose as a potential scaffold for bone regeneration. *Acta Biomater.* **6**, 2540–2547 (2010).

18. Gao, C. *et al.* Preparation and characterization of bacterial cellulose sponge with hierarchical pore structure as tissue engineering scaffold. *J. Porous Mater.* **18**, 139–145 (2011).

19. Uraki, Y., Nemoto, J., Otsuka, H. & Tamai, Y. Honeycomb-like architecture produced by living bacteria , Gluconacetobacter xylinus. *Carbohydr. Polym.* **69**, 1–6 (2007).

20. Tanaka, M., Takebayashi, M., Miyama, M. & Nishida, J. Design of novel biointerfaces (II). Fabrication of self-organized porous polymer film with highly uniform pores. *Biomed. Mater. Eng.* **14**, 439–446 (2004).

21. Reiniati, I., Hrymak, A. N. & Margaritis, A. Kinetics of cell growth and crystalline nanocellulose production by Komagataeibacter xylinus. *Biochem. Eng. J.* **127**, 21–31 (2017).

22. Lee, K. Y., Buldum, G., Mantalaris, A. & Bismarck, A. More than meets the eye in bacterial cellulose: Biosynthesis, bioprocessing, and applications in advanced fiber composites. *Macromol. Biosci.* **14**, 10–32 (2014).

23. Pandey, L. K., Saxena, C. & Dubey, V. Studies on pervaporative characteristics of bacterial cellulose membrane. *Sep. Purif. Technol.* **42**, 213–218 (2005).

24. Bungay, G. S. R. M. H. Inclusion of solid particles in bacterial cellulose. *Appl. Microbiol. Biotechnol.* **58**, 756–760 (2002).

25. Bäckdahl, H., Esguerra, M., Delbro, D., Risberg, B. & Gatenholm, P. Engineering microporosity in bacterial cellulose scaffolds. *J. Tissue Eng. Regen. Med.* **2**, 320–330 (2008).

26. Stumpf, T. R., Yang, X., Zhang, J. & Cao, X. In situ and ex situ modifications of bacterial cellulose for applications in tissue engineering. *Mater. Sci. Eng. C* **82**, 372–383 (2018).

27. Schaffner, M., Rühs, P. A., Coulter, F., Kilcher, S. & Studart, A. R. 3D printing of bacteria into functional complex materials. *Sci. Adv.* **3**, 1–9 (2017).

28. Santos, S. M., Carbajo, J. M. & Villar, J. C. The Effect of Carbon and Nitrogen Sources on Bacterial Cellulose Production and Properties from Gluconacetobacter sucrofermentans CECT 7291 Focused on its use in Degraded Paper Restoration. *BioResources* **8**, 3630–3645 (2013).

29. Rühs, P. A., Storz, F., López Gómez, Y. A., Haug, M. & Fischer, P. 3D bacterial cellulose biofilms formed by foam templating. *npj Biofilms Microbiomes* **4**, 1–7 (2018).

30. Douglass, E. F. *et al.* A Review of Cellulose and Cellulose Blends for Preparation of Bio-derived and Conventional Membranes , Nanostructured Thin Films , and Composites A Review of Cellulose and Cellulose Blends for Preparation of Films , and Composites. *Polym. Rev.* **58**, 102–163 (2018).

31. Gama, M., Gatenholm, P. & Klemm, D. *Bacterial nanocellulose: a sophisticated multifunctional material*. (CRC press, 2012).

32. Burggraaf, A. J. & Cot, L. *Fundamentals of inorganic membrane science and technology*. **4**, (Elsevier, 1996).

33. Joghataei, M., Semnani, D., Salimpour, M. R., Ashrafi, Z. & Khoeini, D. Comparison of heat transfer coefficient for different fabrics by vapor-compression system. *Int. J. Eng. Technol.* **5**, 11–15 (2016).

34. Hernfindez, A., Calvo, J. I., Prfidanos, P. & Tejerina, F. Pore size distributions in microporous membranes . A critical analysis of the bubble point extended method. *J. Memb. Sci.* **112**, 1–12 (1996).

35. Wenten, I. G., Khoiruddin, K., Hakim, A. N. & Himma, N. F. The bubble gas transport method. in *Membrane Characterization* 199–218 (Elsevier, 2017). doi:10.1016/B978-0-

444-63776-5.00011-5

36. Kuo, C. H., Chen, J. H., Liou, B. K. & Lee, C. K. Utilization of acetate buffer to improve bacterial cellulose production by Gluconacetobacter xylinus. *Food Hydrocoll.* **53**, 98–103 (2016).

37. Noro, N., Sugano, Y. & Shoda, M. Utilization of the buffering capacity of corn steep liquor in bacterial cellulose production by Acetobacter xylinum. *Appl. Microbiol. Biotechnol.* **64**, 199–205 (2004).

38. Jang, W. D. *et al.* Genomic and metabolic analysis of *Komagataeibacter xylinus* DSM 2325 producing bacterial cellulose nanofiber. *Biotechnol. Bioeng.* bit.27150 (2019). doi:10.1002/bit.27150

Graphical Abstract

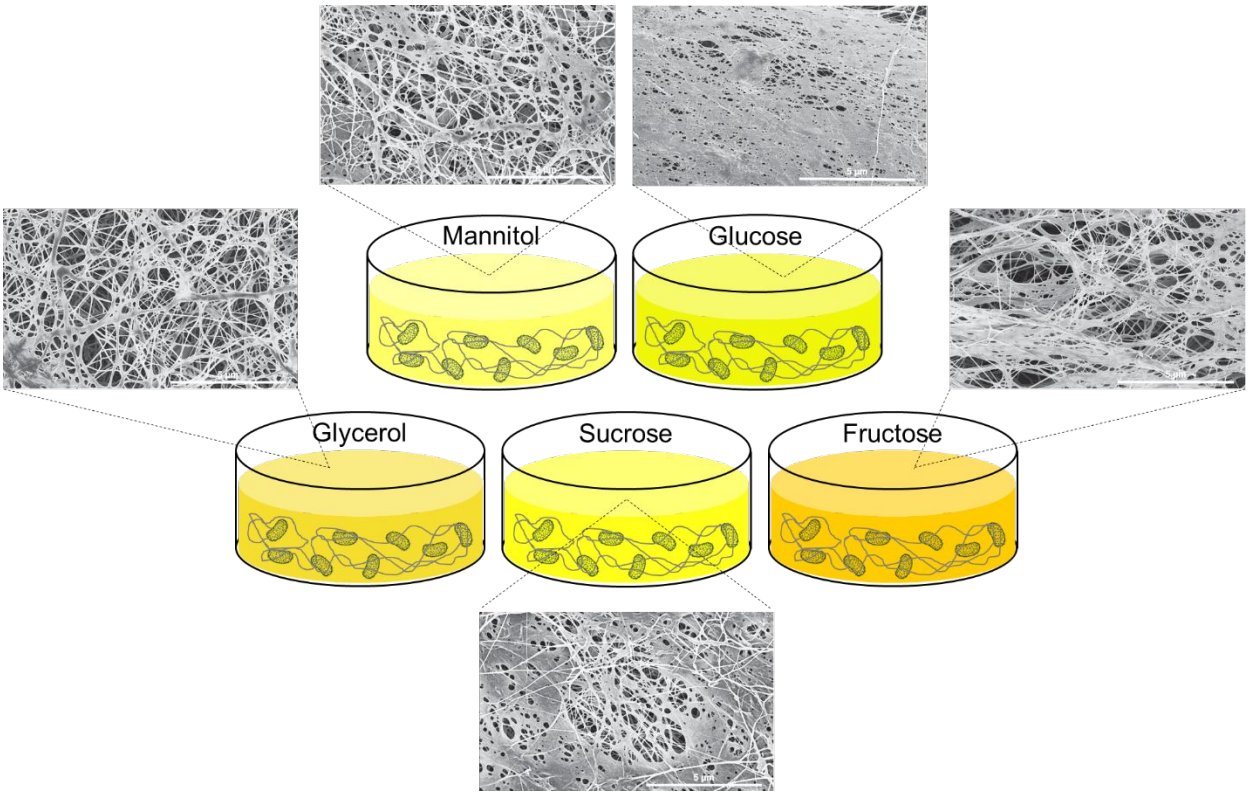

Our work provides the first accounting of how specific culture conditions, i.e., carbon nutrient sources, control morphological and physical properties in bacterial cellulose filaments.